JACC Vol. 24, No. 3
September 1994:784–94

EXPERIMENTAL STUDIES

Surgical Procedure for the Cure of Atrioventricular Junctional ("AV Node") Reentrant Tachycardia: Anatomic and Electrophysiologic Effects of Dissection of the Anterior Atrionodal Connections in a Canine Model

MARK A. McGUIRE, PhD, FRACP,* ALEX S. B. YIP, MRCP, MONICA ROBOTIN, MB, JOHN P. BOURKE, MRCP, DAVID C. JOHNSON, FRACS, BARBARA I. DEWSNAP, RICHARD CHARD, FRACS, JOHN B. UTHER, MD, FRACP, DAVID L. ROSS, FRACP, FACC

Sydney, New South Wales, Australia

Objectives. **This study was undertaken to examine the electrophysiologic and anatomic effects of a surgical procedure that cures the anterior (common) type of atrioventricular (AV) junctional reentrant tachycardia.**

Background. **The procedure was designed to interrupt the reentrant circuit at the point of earliest atrial activation during AV junctional reentrant tachycardia, the anterior atrionodal connections.**

Methods. **Atrioventricular node function and the sequence of electrical excitation of Koch's triangle were examined in 18 dogs. Excitation of Koch's triangle was mapped using a 60-channel mapping system. Surgical dissection was performed in 10 dogs and a sham procedure in 8. After 28 to 35 days, AV node function and the atrial excitation pattern were reassessed. The AV junction was examined using light microscopy.**

Results. **Some degree of AV node damage was visible in all dogs in the dissection group, but it was minor in 40% of cases. The anterior part of the AV node was disconnected from the anterior atrionodal connections in all cases. Anterograde AV node function was mildly impaired. The median AH interval was increased (62 vs. 76 ms [interquartile ranges 48 to 72 and 64 to 104, respectively], $p = 0.05$), and the AV Wenckebach cycle length was increased (210 vs. 245 ms [interquartile ranges 200 to 230 and 210 to 260, respectively], $p = 0.02$). The degree of impairment of conduction was directly proportional to the length of dissection ($p < 0.05$) but not to the degree of damage to the AV node. Ventriculoatrial (VA) conduction was destroyed in 50% of dogs undergoing dissection but in none of those with a sham operation ($p < 0.04$). The AV node remained responsive to autonomic blocking drugs, and atrial mapping during ventricular pacing revealed that the site of exit from the AV node had been altered.**

Conclusions. **The atrionodal connections closest to the His bundle are the preferred route of conduction through the AV node during normal AV or VA conduction. Destruction of these connections modifies AV node conduction. The surgical procedure selectively interrupts these connections, and this interruption is likely to be the mechanism of cure.**

(J Am Coll Cardiol 1994;24:784–94)

Atrioventricular (AV) junctional reentrant tachycardia, a frequent cause of supraventricular tachycardia, is due to reentry in the region of the AV node (1–3). Recent investigations (4–10) suggest that perinodal atrial tissue forms part of the reentrant circuit. In 1983 we (4) developed a surgical procedure for the cure of AV junctional reentrant tachycardia. Based on the premise that atrial tissue participated in the reentrant circuit, this procedure was designed to interrupt the reentrant circuit at the point of exit from the AV node. Intraoperative mapping of the "common" or anterior type of AV junctional reentrant tachycardia had revealed that the site of earliest atrial activation during this tachycardia was near the apex or anterior end of Koch's triangle (4,11). Accordingly, the surgical procedure was designed to destroy the anterior connections between the AV node and the atrium, leaving the posterior connections intact. Similarly, AV junctional reentrant tachycardia may be cured by lesions placed at this site using the recently developed technique of catheter ablation (12,13).

The operative procedure has a high success rate and a low mortality rate (4,14). However, it has not been possible to confirm the histologic effects of the dissection or the mechanism of cure because human tissue cannot be obtained for microscopic examination. The aim of the current study was to

From the Cardiology Department, Westmead Hospital, Sydney, New South Wales, Australia. This work was supported in part by a grant-in-aid from the National Heart Foundation of Australia, Woden, Australian Capital Territory, Australia. Dr. McGuire is the recipient of a Postgraduate Medical Research Scholarship from the National Health and Medical Research Council of Australia, Canberra, Australian Capital Territory. Dr. Bourke was the 1989 Anglo-Australian Fellow of the British Heart Foundation, London, England. Telectronics, Australia provided pacemakers and pacing leads.

*Present address: Department of Cardiology, Royal Prince Alfred Hospital, Missenden Road, Camperdown, New South Wales 2050, Australia.

Manuscript received April 2, 1993; revised manuscript received April 11, 1994, accepted April 21, 1994.

Address for correspondence: Dr. David L. Ross, Cardiology Unit, Westmead Hospital, Westmead, New South Wales 2145, Australia.

©1994 by the American College of Cardiology

0735-1097/94/$7.00

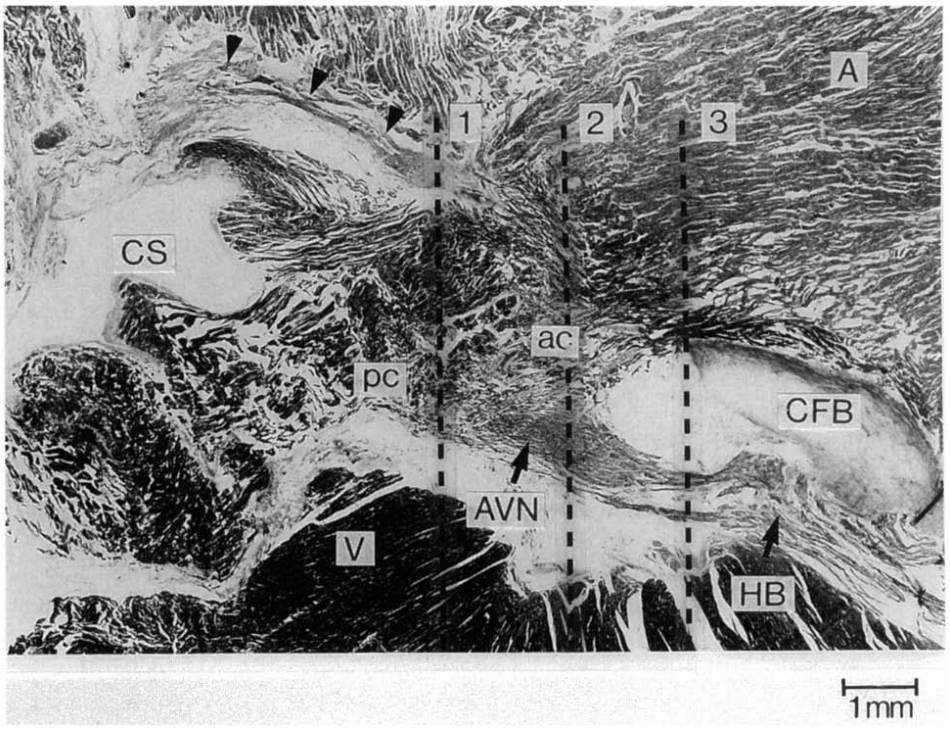

Figure 1. Section showing the positions of the anterior (ac) and posterior (pc) atrionodal connections and of the sections used in subsequent figures (**dashed lines 1 to 3**). The plane of section is parallel to the cardiac septum, which is perpendicular to subsequent sections. **Arrowheads** indicate the tendon of Todaro. A = atrial myocardium; AVN = AV node; CFB = central fibrous body; CS = coronary sinus; HB = bundle of His; V = ventricular septum.

examine the anatomic and electrophysiologic effects of the surgical procedure in an animal model.

Methods

Overview of protocol. The protocol was approved by the Westmead Hospital Animal Research and Ethics Committee. Electrophysiologic characteristics, both in the baseline state and after the administration of autonomic blocking drugs, were examined in 18 dogs with the use of standard percutaneous techniques. The animals were then placed on cardiopulmonary bypass, and electrical activation of Koch's triangle and proximal coronary sinus was examined using a multichannel mapping system. Surgical dissection was performed in 10 dogs and a sham procedure in 8. After 28 to 35 days a second electrophysiologic study was performed to assess changes in AV node function, and 1 week later repeat mapping of electrical activation was performed to assess changes in the routes of AV and ventriculoatrial (VA) conduction. The animals were then killed, and the AV junction was examined with light microscopy.

Terminology. *Anterior atrionodal connections* are defined as the atrial or transitional fibers approaching the AV node from the anterior atrial septum, predominantly from the anterior limbus of the fossa ovalis (Fig. 1). These fibers are equivalent to the combined "superficial" and "deep" transitional cell groups of Becker and Anderson (15). Posterior atrionodal connections are defined as transitional or atrial fibers approaching the AV node from the region between the coronary sinus orifice and tricuspid annulus and from the region between the coronary sinus and inferior vena cava orifice (the "sinus septum"). These are equivalent to the posterior group of transitional cells of Becker and Anderson (15). *Compact node* is defined as the area of the AV node composed of tightly packed and interweaving cells (15); it is equivalent to the area of the Knotenpunkten described by Tawara (16).

Electrophysiologic study. In male or female adult mongrel dogs weighing 16 to 37 kg, anesthesia was induced with sodium thiopentone (20 mg/kg body weight intravenously). After endotracheal intubation, anesthesia was maintained with halothane (1.5% to 2.0%) and a 2:1 mixture of nitrous oxide and oxygen. Electrode catheters were introduced under fluoroscopic control through the right femoral vein, to the high right atrium and the right ventricular apex for recording and pacing. A tripolar electrode catheter was placed across the tricuspid valve ring to record signals from the His bundle. Recordings were made using an eight-channel recorder (Siemens-Elema Mingograf) at paper speeds of 100 and 250 mm/s, using a band-pass of 30 to 500 Hz.

Anterograde AV conduction was assessed using extrastimulus testing and incremental pacing. Extrastimulus testing was performed using two basic drive cycle lengths, set as close as possible to 350 and 300 ms. Single atrial extrastimuli were delivered after drive trains of 8 to 15 beats with intervals of 3 s separating successive trains. The coupling interval of the initial extrastimulus was 10 ms less than the drive cycle length, and successive coupling intervals were shortened in 10-ms decrements until atrial refractoriness. In all cases the coupling intervals of atrial extrastimuli (A_1A_2) were plotted against the AH interval (A_2H_2), and the curve was examined for the presence of discontinuities that would suggest the presence of dual anterograde AV node pathways. Incremental pacing was commenced at a cycle length 30 ms less

than the sinus cycle length and then increased until second-degree AV block occurred.

Retrograde conduction was assessed in an analogous manner using ventricular stimulation. Coupling intervals of ventricular extrastimuli (V_1V_2) were plotted against corresponding VA intervals (V_2A_2), and the curve was examined for the presence of discontinuities that would suggest the presence of dual retrograde AV node pathways.

After completion of this stimulation protocol, atropine (0.4 mg/kg, 1 mg/min) then propranolol (0.2 mg/kg, 1 mg/min intravenously) were administered to induce blockade of the autonomic nervous system. The stimulation protocol was then repeated using drive cycle lengths as close as possible to those used in the baseline state. The purpose of inducing autonomic blockade was 1) to enable comparison of preoperative and postoperative AV node function without the confounding influence of autonomic tone, which might vary between the two studies, and 2) to allow assessment of the effects of the operative procedure on the autonomic innervation of the AV junction.

A second (postoperative) electrophysiologic study was performed 28 to 35 days after the operative procedure using a protocol identical to that used at the first study. If VA conduction was not demonstrable, isoproterenol was administered intravenously in successive bolus doses of 2, 4 and 6 μg, and the capacity for VA conduction was reassessed after each dose.

Surgical procedure. After intramuscular premedication with both morphine (1 mg/kg) and atropine (0.04 mg/kg), anesthesia was induced with sodium thiopentone (20 mg/kg intravenously). The dog was intubated and ventilated with a tidal volume of 20 ml/kg. Anesthesia was maintained with halothane (1.5% to 2.5%) and a 2:1 nitrous oxide–oxygen mixture. Morphine (1 to 2 mg/kg intravenously) and pancuronium (0.04 mg/kg intravenously) were administered before either dissection or the sham procedure was started.

A thoracotomy was made in the right fifth intercostal space, and the heart was suspended in a pericardial sling. Cannulas were placed in the left femoral artery and the superior and inferior venae cavae for cardiopulmonary bypass. The oxygenator and tubing were primed with heterologous blood. A plaque electrode was introduced through an oblique incision in the anterolateral right atrium for operative mapping of the region surrounding the AV node. Normothermia was maintained during the mapping period. On completion of mapping, the ascending aorta was cross-clamped, and a cardioplegic solution was infused into the aortic root.

After arrest of the heart, either dissection of the anterior atrionodal connections or a sham procedure was performed (see later). Then the atriotomy was closed, the aortic cross-clamp removed and the heart defibrillated. A ventricular-inhibited (VVI) permanent pacemaker (Optima, Telectronics, Lane Cove, New South Wales, Australia) was implanted in dogs in the anterior dissection group. Pacemakers were implanted because *temporary* AV block is frequently observed for some days in humans undergoing this procedure. After the chest wall was closed, the intercostal nerves in the region of the thoracotomy were infiltrated with bupivacaine (0.5%) to provide postoperative analgesia, and supplementary morphine was administered subcutaneously as required.

Dissection technique. This procedure has been described in detail elsewhere (4,14). In summary, stay sutures were placed in the tricuspid annulus, and the right atrial endocardium was incised just above the tricuspid annulus. This incision extended from the central fibrous body to a point posterolateral to the coronary sinus orifice. The right atrial endocardium was then peeled back to expose the posterior septal space. With a scalpel the anterior atrial connections of the AV node were separated from the node from a point just behind the central fibrous body. The dissection was continued posteriorly for 3 to 4 mm and medially toward the mitral annulus until that structure was identified. The posterior connections of the AV node were left intact. In dogs undergoing the sham procedure, operative mapping was performed, the aortic cross-clamp was applied and cardioplegic solution infused, but no dissection was performed. The aortic cross-clamp was removed after 15 min.

Mapping of atrial activation. Electrodes were placed on the right ventricular outflow tract and the right atrial appendage to pace these chambers. A 60-electrode mapping plaque, similar to that described previously, was introduced through an oblique incision in the anterolateral wall of the right atrium (11). The unipolar electrodes were arranged in a polygonal array with a 2-mm interelectrode distance; 56 electrodes were apposed to the endocardial surface overlying Koch's triangle, and the surrounding atrium and 4 electrodes were positioned along a process that extended from the surface of the plaque into the coronary sinus. Leads I, aVF and V_1 or V_2 were used to record the surface electrocardiogram. After the mapping plaque was positioned, the ventricles were paced, and extrastimuli were delivered after drive trains of 8 beats. The first coupling interval was 40 ms less than the drive cycle length, and subsequent coupling intervals were decreased in steps of 40 ms. Intervals of 3 s separated successive drive trains. If VA conduction was not present in the baseline state, bolus injections of isoproterenol (successive doses of 2, 4, 6 and 8 μg intravenously) were administered, and the capacity for VA conduction was assessed after each dose.

A second mapping procedure was performed 28 to 35 days after the first operative procedure. The anesthetic and mapping techniques used were identical to those used at the first procedure, except that the oxygenator used for cardiopulmonary bypass was primed with saline solution rather than blood.

Signal processing and analysis. These methods have been described previously (11). In brief, signals were recorded during sinus rhythm and ventricular pacing with a gain of 500 to 1,000 and bandpass of 0.2 to 500 Hz. An optional high pass (−3 dB point 35 Hz) was used for some of the recordings. The point of maximal negative dV/dt of electrograms was assumed to represent the time of local activation. Isochrone maps were constructed by joining points activated simultaneously.

Histologic examination. At the completion of the second mapping study, sodium pentobarbitone was administered (160 mg/kg intravenously). After cessation of cardiac activity,

the heart was removed and fixed in a solution of 10% formalin. A block of tissue containing the AV junction in the region of the septum was excised. The anterior limit of the tissue block was anterior to the central fibrous body, and the posterior limit was the epicardium overlying the posterior septal space. The block was divided into slices of ~5 mm and embedded in paraffin. The plane of section was perpendicular to the plane of AV rings and perpendicular to the plane of the interatrial septum. Sections of 5-μm thickness were cut, and every 10th section was stained with Gomori trichrome and examined with light microscopy. The atrionodal connections were recognized by their position adjacent to the compact AV node and the cellular characteristics of transitional cells as described by Tawara (16) and Becker and Anderson (15).

Damage to the compact AV node was assessed using a four-level scoring system: level 0 = no visible damage to the AV node; level 1+ = possible minor damage to the compact node, scar tissue adjacent to the edge of the compact node but no visible infiltration of the compact node; level 2+ = scar tissue encroaching on the compact node but no damage to large bundles of nodal tissue; level 3+ = marked encroachment of the node by scar tissue with small scattered bundles of nodal tissue surviving. Two observers assessed the degree of AV node damage independently. The length of the dissection is defined as the distance from the most anterior point at which transitional cells contacted the compact AV node to the point where the compact node entered the central fibrous body.

Statistical analysis. Unless otherwise stated, group data with a nonnormal distribution are expressed as the median value, and the interquartile range is given in parentheses. The Wilcoxon and Mann-Whitney tests were used for comparison. Normally distributed data are expressed as mean value ± SD, and the *t* test was used for comparison. Examination of the relation between histologic changes and impairment of AV conduction was performed by using simple regression and the Spearman rank test. Analysis was performed with the use of a commercially available software package (StatView II, Abacus Concepts).

Results

Histologic examination. In all cases the most distal of the anterior atrionodal connections were destroyed, and a band of fibrous tissue separated the anterior part of the compact AV node from overlying atrium (Figs. 1 to 4). The mean length ± SD of the dissection was 2.0 ± 1.0 mm (range 0.9 to 3.5). The posterior approaches to the AV node (Fig. 2) remained intact in all cases. The degree of histologic damage to the AV node was variable. In six cases (60%) grade 2+ or 3+ infiltration of the compact node by scar tissue had occurred. In the cases with most severe AV node damage, only a few scattered viable AV node cells were present. In some of these cases, despite marked fibrosis of the compact AV node, the capacity for anterograde and retrograde conduction remained excellent. In the remaining four cases (40%) we judged the degree of AV node damage to be minor (grade 1+). In these four cases scar tissue was present adjacent to the distal compact AV node,

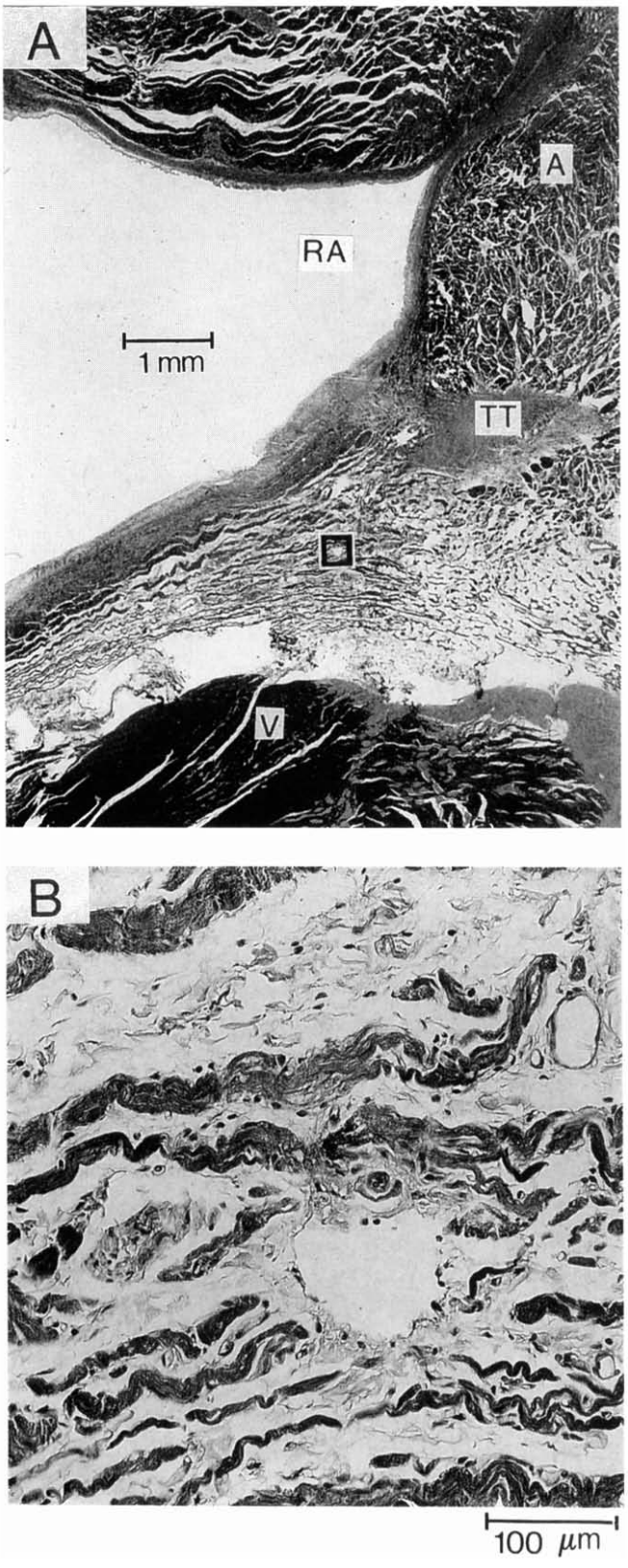

Figure 2. A, Posterior atrionodal connections after anterior atrionodal dissection. The posterior connections are undamaged. The section is cut perpendicular to the atrioventricular groove, its position indicated by **dashed line 1** in Figure 1 (level of the fossa ovalis). **The small square** indicates the region shown in **B. B, High** magnification view of posterior atrionodal connections showing undamaged cells of the transitional type. A = atrial septum; RA = cavity of right atrium; TT = tendon of Todaro; V = ventricular septum.

JACC Vol. 24, No. 3
September 1994:784–94

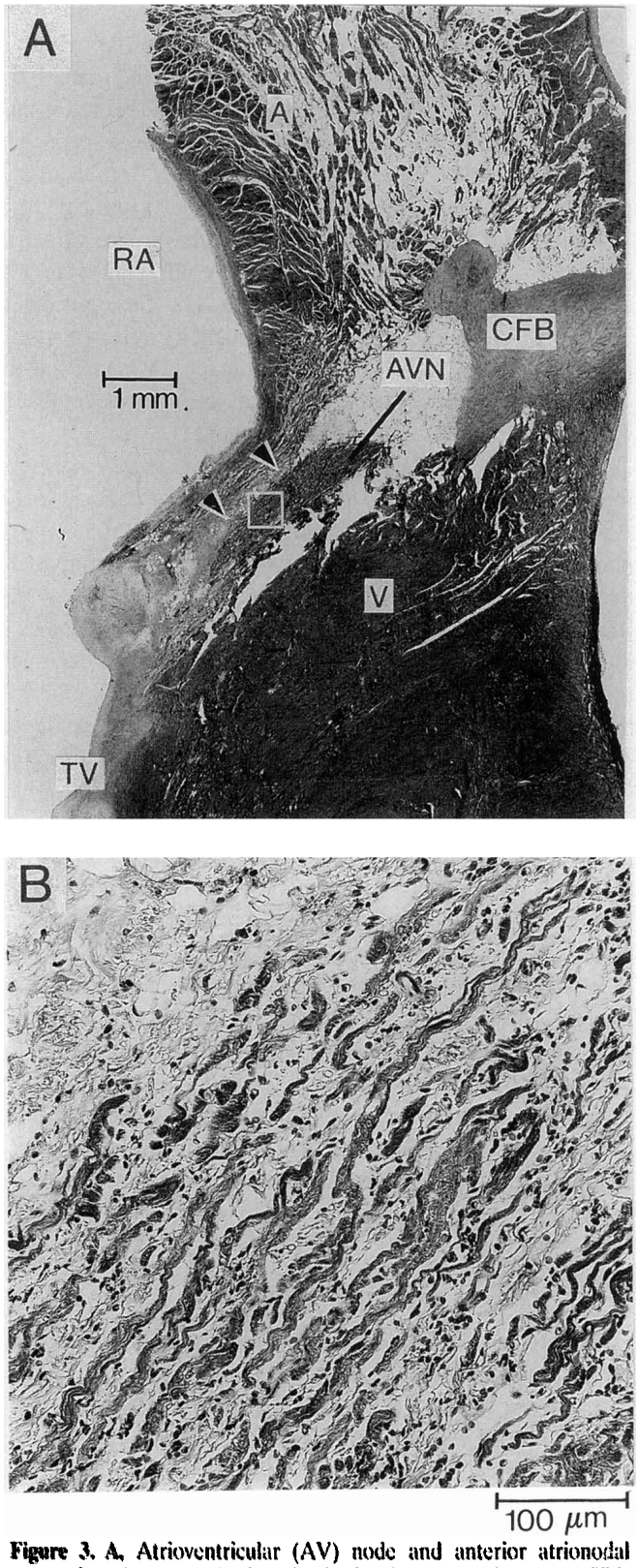

Figure 3. A, Atrioventricular (AV) node and anterior atrionodal connections **(arrowheads)** in a dog in the sham operation group. This figure has been included for comparison with Figure 4. The section is cut perpendicular to the AV groove, its position indicated by **dashed line 2** in Figure 1. The **small square** indicates the region shown in **B. B,** High magnification view of the compact AV node. The transitional cells of the atrionodal connections are shown at **upper left** and compact nodal cells at **lower right.** A = medial wall of right atrium; Ao = aorta; TV = septal leaflet of tricuspid valve; other abbreviations as in Figures 1 and 2.

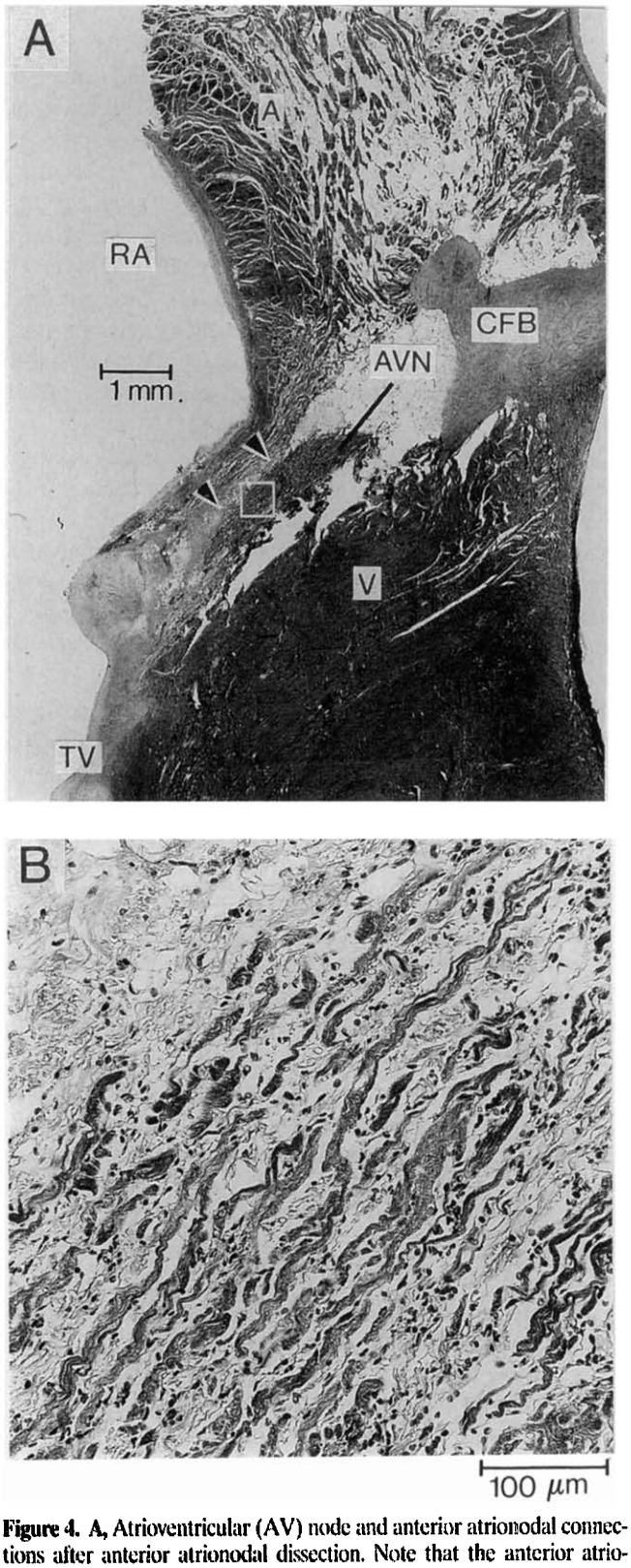

Figure 4. A, Atrioventricular (AV) node and anterior atrionodal connections after anterior atrionodal dissection. Note that the anterior atrionodal connections have been destroyed and that the AV node is separated from the overlying atrium by a band of fibrous tissue (indicated by **arrowheads**). The section is cut perpendicular to the AV groove, its approximate position indicated by **dashed line 2** in Figure 1. The **small square** indicates the region shown in **B. B,** High magnification view of the compact AV node. The anterior atrionodal connections are replaced by fibrous tissue **(upper left)** that separates the AV node from the atrium. There is some increase in fibrous tissue in the periphery of the compact AV node **(middle and lower right).** Abbreviations as in Figures 1 to 3.

Table 1. Effect of Anterior Atrionodal Dissection on Anterograde Conduction (measured after autonomic blockade)

	Preoperative (n = 10)	Postoperative (n = 10)	p Value
Sinus CL	446 (396–508)	446 (412–496)	0.84
PA interval	32 (32–36)	30 (24–32)	0.03*
AH interval			
Sinus rhythm	62 (48–72)	76 (64–104)	0.05†
Atrial pacing, CL 300 ms	80 (80–90)	95 (80–140)	0.05†
HV interval	28 (28–32)	28 (28–28)	0.32
QRS duration	54 (52–60)	56 (52–60)	1.00
AV Wenckebach CL‡	210 (200–230)	245 (210–260)	0.02†
AV node relative refractory period	275 (260–280)	280 (270–280)	0.17
AV node functional refractory period	250 (240–260)	255 (240–280)	0.40

*Although the change in PA interval is statistically significant, a change of 2 ms is within the measurement error and therefore is not meaningful. †Statistically significant value. ‡Longest cycle length (CL) of atrial pacing inducing second-degree atrioventricular (AV) block. Values are expressed in ms as median value (interquartile range). The drive cycle length was 300 ms.

which appeared undamaged, but some minor damage to cells in the periphery of the compact node could not be excluded (Fig. 4). The His bundle was undamaged in all cases except one in which moderate infiltration by scar tissue was present. The postoperative HV interval was unchanged from the preoperative value in this case.

Electrophysiologic studies. The results of electrophysiologic studies are summarized in Tables 1 to 4. The results were similar for both basic drive cycle lengths, and thus results are tabulated only for the 300-ms drive cycle length.

Effect of dissection on echo beats. Before dissection, narrow complex AV junctional echo beats were induced by ventricular pacing in 8 (80%) of the 10 dogs in the dissection group. Postoperatively, echo beats were present in four (50%) of these eight dogs. In the four dogs in which echo beats were abolished, VA conduction had been destroyed. In the dogs in the sham operation group, echo beats were present in seven (88%) of eight dogs preoperatively and in the same number of dogs postoperatively. Atrioventricular junctional echo beats could not be induced by atrial pacing in any dog in either the preoperative or the postoperative studies.

Effect of dissection on anterograde AV node conduction. When assessed under basal conditions the dissection had no significant effect on anterograde conduction. When assessed under autonomic blockade, however, dissection caused small but significant changes (Tables 1 and 2). Significant prolongation of the AH interval was observed, and Wenckebach-type AV block occurred at lower rates of atrial pacing. The AV node relative and functional refractory periods were not altered. Significant changes in the A_2H_2 interval during atrial extrastimulus testing were observed when the A_1A_2 interval was ≥260 ms but not at shorter coupling intervals.

Before the operative procedure, dual anterograde AV node pathways were not detected during extrastimulus testing or incremental pacing in any dog. The AV node effective refractory period could not be measured in 17 of the 18 dogs because anterograde AV conduction was limited by refractoriness in the atrium rather than in the AV node. Apart from a minor

Table 2. Effect of Anterior Atrionodal Dissection on Anterograde Conduction in Dissection Group Versus Sham Operation Group (measured after autonomic blockade)

	Sham Operation (n = 8)	Dissection (n = 10)	p Value
Sinus CL	426 (398–442)	446 (412–496)	0.23
PA interval	35 (30–42)	30 (24–32)	0.15
AH interval			
Sinus rhythm	58 (50–64)	76 (64–104)	0.03*
Atrial pacing, CL 300 ms	65 (60–80)	95 (80–140)	0.03*
HV interval	28 (24–30)	28 (28–28)	0.70
QRS duration	54 (48–60)	56 (52–60)	0.56
AV Wenckebach CL	205 (190–230)	245 (210–260)	0.05*
AV node relative refractory period	270 (260–280)	280 (270–280)	0.24
AV node functional refractory period	235 (225–255)	255 (240–280)	0.56

*Statistically significant value. Values are expressed in ms as median value (interquartile range). The drive cycle length was 300 ms. Abbreviations as in Table 1.

Table 3. Effect of Autonomic Blocking Drugs on Anterograde Conduction After Anterior Atrionodal Dissection

	Basal State (n = 10)	After Autonomic Blockade (n = 10)	p Value
Sinus CL	400 (316–464)	446 (412–496)	0.02*
PA interval	28 (28–32)	30 (24–32)	0.58
AH interval			
Sinus rhythm	58 (48–80)	76 (64–104)	0.01*
Atrial pacing, CL 300 ms	70 (60–110)	95 (80–140)	0.01*
HV interval	28 (28–28)	28 (28–28)	NS
QRS duration	56 (52–60)	56 (52–60)	0.31
AV Wenckebach CL	205 (190–220)	245 (210–260)	0.02*
AV node relative refractory period	270 (260–280)	280 (270–280)	0.09
AV node functional refractory period	230 (220–250)	255 (240–280)	0.06

*Statistically significant result. Values are expressed in ms as median value (interquartile range). The drive cycle length was 300 ms. Abbreviations as in Table 1.

change in the median AV node relative refractory period (275 ms [range 255 to 285] vs. 245 ms [range 225 to 265], p = 0.03), the sham procedure had no effect on anterograde conduction, either in the basal state or after autonomic blockade. Before the operative procedure, anterograde conduction in the sham operation group was comparable to that of the dissection group under basal conditions and under autonomic blockade.

Autonomic blocking drugs retained significant effects on anterograde AV node conduction when assessed 4 to 5 weeks after anterior dissection (Table 3), suggesting that the procedure had not caused autonomic denervation of the AV node.

Effect of the operative procedure on VA conduction during ventricular pacing. The effect of the operative procedure on VA conduction was assessed under basal conditions and under autonomic blockade. However, although all dogs manifested 1:1 VA conduction in the baseline state, autonomic blockade prevented VA conduction in five (63%) of the sham operation group and 6 (60%) of the dissection group preoperatively. Thus, the number of dogs with intact VA conduction after autonomic blockade was too small for statistically meaningful analysis of the effects of surgery; accordingly, only the results measured under basal conditions are presented (Table 4).

Ventriculoatrial conduction was lost in 5 of the 10 dogs after anterior dissection ($p < 0.04$) but in none of the sham operation group. When the characteristics of postoperative VA conduction in the five dogs with intact conduction were compared with preoperative values in the same dogs, the VA effective refractory period and the shortest paced cycle length with 1:1 conduction were both shortened (Table 4). The VA interval did not increase after dissection; the sham procedure had no effect on VA conduction. Discontinuities in the curve V_1V_2 versus V_2A_2 indicative of the presence of dual retrograde AV node pathways were not present in any dog at the percutaneous electrophysiologic study. However, dual retrograde AV node exits (indicating the presence of dual pathways) were detected in some dogs in the intraoperative mapping studies (see later).

Table 4. Effect of Anterior Atrionodal Dissection on Ventriculoatrial Conduction (measured under basal conditions)

	Preoperative (n = 5)*	Postoperative (n = 5)*	p Value
VA interval†	130 (100–200)	150 (105–163)	0.50
VA effective refractory period	280 (243–305)	210 (188–275)	0.04‡
VA relative refractory period	340 (310–353)	330 (258–380)	1.0
VA functional refractory period	340 (303–355)	310 (213–338)	0.07
VA Wenckebach cycle length	340 (293–373)	310 (218–348)	0.04‡

*Only five dogs are included because dissection abolished ventriculoatrial (VA) conduction in the remaining five dogs. †Measured during the drive cycle (cycle length 400 ms). ‡Statistically significant result. Values are expressed in ms as median value (interquartile range).

Mapping of atrial activation. *Sinus rhythm.* During sinus rhythm, excitation approached Koch's triangle along the anterior limbus, and the anterior atrionodal connections were activated before the posterior atrionodal connections. The dissection did not alter the pattern of atrial excitation during sinus rhythm.

Ventricular pacing. Before dissection, the site of exit from the AV node during ventricular pacing was assessed using the plaque electrode and computerized mapping system. A single anterior site of exit, located at the apex of Koch's triangle at the site of the anterior atrionodal connections, was noted in seven dogs. In two dogs, dual exits similar to those previously described in humans (4,11,17) were observed. These dual exits were anatomically correlated, respectively, with the sites of the anterior and posterior atrionodal connections (Fig. 1). In these two dogs, drive cycle stimuli were conducted over a "fast pathway" that first activated the atria through the anterior exit, close to the His bundle. However, closely coupled ventricular extrastimuli were conducted to the atria by way of a "slow" pathway. The site of the latter exit was posterior to the AV node, near the orifice of the coronary sinus, at the site of the posterior atrionodal connections. In one dog only a posterior exit was observed. Thus, it was possible to assess the effects of the operative procedure on the anterior exit in 9 of the 10 dogs.

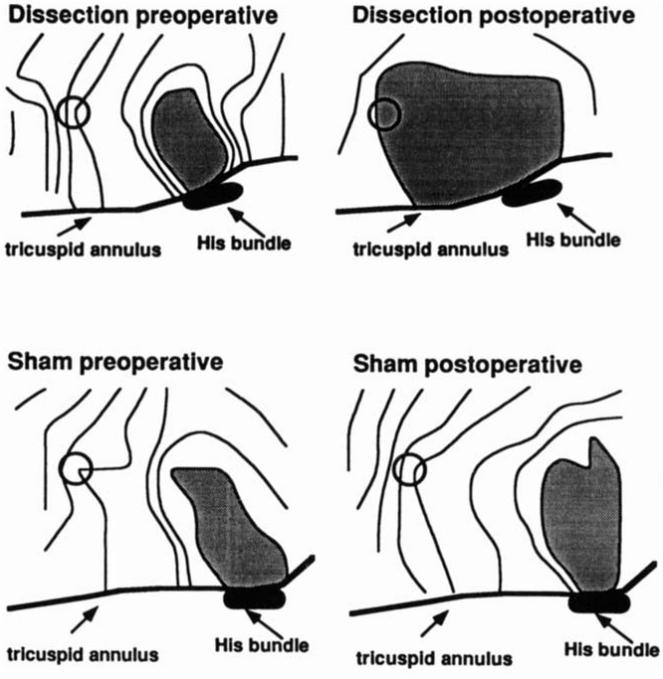

Figure 5. Maps of excitation of Koch's triangle and surrounding region during ventricular pacing. Isochrones are drawn at 2-ms intervals. The **circles** mark the position of the coronary sinus orifice. The **shaded areas** indicate the site of earliest atrial excitation. The **upper panels** show the effect of dissection in a single dog. The area enclosed by the 2-ms isochrone is much larger in the postoperative map (**right**) than in the preoperative map (**left**). No significant change was observed in dogs in the sham operation group (**lower panels**).

Although VA conduction was present in only 5 dogs (50%) in the dissection group at the second percutaneous electrophysiologic study, it was present in eight dogs (80%) at the second mapping study. Presumably, the increased sympathetic tone induced by cardiopulmonary bypass permitted VA conduction in the three additional dogs. An anterior exit had been demonstrated in seven of these dogs at the preoperative study. This exit was altered by the dissection in six cases (86%). In one case, the anterior exit was destroyed, and only the posterior exit remained; in the remaining five cases, the site of earliest atrial activation was spread over a larger area so that almost the entire triangle of Koch was activated simultaneously (Fig. 5). In these dogs the mean value ± SD of the area enclosed by the isochrone encircling the initial 2 ms of atrial activation was 12 ± 10 mm^2 at the preoperative study and 46 ± 13 mm^2 at the postoperative study ($p < 0.005$, paired *t* test). This change appeared to be due to the site of the atrial exit, which was deeper in the atrial septum and thus allowed the wave front of excitation to spread transversely before reaching the right atrial endocardium (Fig. 6). In the sham operation group we observed no significant change in the site of the atrial exit or in the size of the area enclosed by the 2-ms isochrone (19 ± 12 vs. 20 ± 8 mm^2, $p = 0.74$). Thus, the operative dissection either altered the site of exit from the AV node or abolished VA conduction completely in eight (88%) of the nine dogs in which it could be assessed.

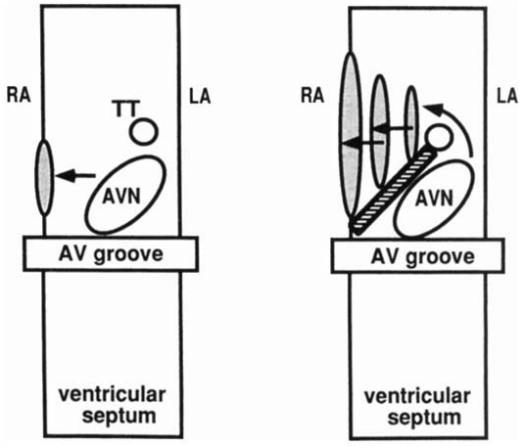

Figure 6. Postulated mechanism of dissection-induced change in atrial excitation during ventricular pacing. **Left,** Before dissection, excitation (**shaded ellipse**) spreads directly from the atrioventricular (AV) node to the right atrial endocardium by way of superficial atrionodal connections. **Right,** After dissection, the AV node is insulated from endocardium by fibrous tissue (**hatched area**). Activation exits from the AV node by way of connections close to the left side of the septum. This allows the impulse to spread radially before it reaches the right atrial endocardium. Thus, the area of earliest atrial excitation is larger postoperatively. LA = left atrium; RA = right atrium; other abbreviations as in Figures 1 and 2.

Correlation between anatomic lesions and changes in AV conduction. Changes in anterograde AV node function correlated directly with the length of dissection (Fig. 7). Both the postoperative AH interval and the percent change in the anterograde Wenckebach point correlated positively with the length of dissection ($r = 0.70$, $p = 0.02$ and $r = 0.70$, $p < 0.03$, respectively). No significant correlation was found between the degree of direct AV node damage and changes in anterograde AV node function ($p = 0.8$).

Loss of VA conduction was associated with both severe AV node damage and more extensive destruction of the anterior atrionodal connections. Of the five dogs without VA conduction at the postoperative electrophysiologic study, four had

Figure 7. Correlation between the length of dissection and the postoperative AH interval (measured under autonomic blockade, with atrial pacing at a cycle length of 300 ms).

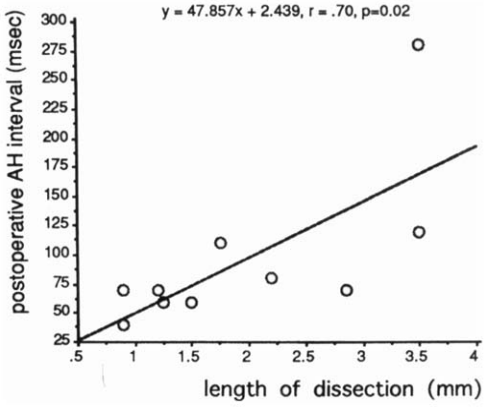

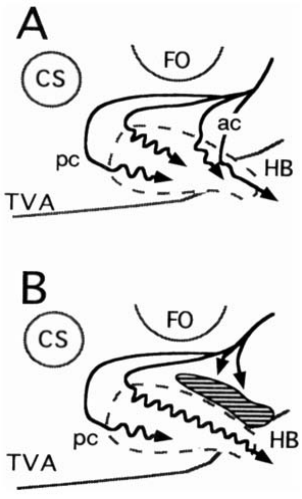

Figure 8. Postulated mechanism of increase in AH interval after dissection of anterior atrionodal connections. **A,** During sinus rhythm in the normal heart, activation proceeds by way of the anterior limbus of the fossa ovalis (FO) and enters the atrioventricular (AV) node by way of anterior atrionodal connections. **B,** After dissection (**hatched area**), the impulse can no longer enter the anterior connections and must enter the AV node by way of posterior connections. The **dashed line** indicates the compact AV node. CS = coronary sinus orifice; TVA = tricuspid annulus; other abbreviations as in Figure 1.

marked AV node fibrosis but one had only minor AV node damage. The length of dissection was longer in dogs that lost VA conduction than in those that did not (mean ± SD 2.6 ± 1.0 mm vs. 1.3 ± 0.3 mm, $p = 0.03$).

Microscopic examination showed that, in dogs whose pattern of atrial activation was altered by dissection, the most anterior of the residual intact atrionodal connections (i.e., those closest to the His bundle) were close to the mitral valve annulus. In the one dog whose pattern of atrial activation was unchanged, the most anterior of the intact atrionodal connections was close to the right atrial endocardium. This location explains the lack of change in the pattern of activation in this dog because a change in a superficial site of exit of only 1 to 2 mm would be beyond the resolution of our recording system.

Discussion

This study confirms that the surgical procedure achieved its aim of sectioning the distal anterior atrionodal connections, leaving the posterior atrionodal connections intact (Fig. 8). The AV node suffered significant structural damage in 60% of cases. Despite the degree of structural damage, anterograde AV node function was well preserved, with only small increases in the AH interval and AV Wenckebach point. Retrograde AV node function was markedly impaired in 50% of cases, and the site of exit from the AV node during VA conduction was altered.

These findings are consistent with the changes in AV node function observed in humans undergoing curative surgical procedures. Previous studies have reported that anterograde AV node function is well preserved and that retrograde AV node conduction block is induced in 0% to 25% of cases (4,5,8,18). Small increases in the AH interval, similar to those found in the present study, were observed by Ross et al. (4).

Mechanism of cure of AV junctional reentrant tachycardia. Studies performed in humans have not revealed a consistent mechanism of surgical cure of AV junctional reentrant tachycardia. It is not necessary to abolish retrograde conduction nor to destroy either of the dual AV node pathways to achieve cure of tachycardia (4,8,19). Several studies (8,14) have reported that AV node echo beats could be induced postoperatively in patients cured of AV junctional reentrant tachycardia. Residual reentrant circuits incapable of sustained reentry are therefore quite frequent.

The current study does not determine with certainty whether the site of the curative lesion is intranodal or extranodal. It is likely, however, that cure is due to lesions of the anterior atrionodal connections because these were destroyed in all cases, whereas significant AV node damage was observed in only 60% of cases. Because the cure rate for this type of surgery is 85% to 100%, it is unlikely that direct AV node damage is responsible for cure (4,14,18,19). However, we cannot exclude the possibility that minor AV node damage occurred more frequently than was detected with light microscopy, although this is unlikely in view of the relatively slight impairment of AV node function.

Denervation of the AV node is unlikely to be the mechanism of cure. Postoperative administration of autonomic blocking drugs caused significant impairment of AV conduction, indicating that sympathetic innervation of the AV node was intact. Moreover, it is unlikely that parasympathetic denervation had been produced because postoperative AV conduction was mildly impaired, whereas parasympathetic denervation would have facilitated conduction. This finding is in agreement with that of Fujimura et al. (8), who found intact autonomic innervation in patients in whom curative surgery had been performed. The surgical procedure used by the latter investigators was more extensive than that used in the present study because both anterior and posterior AV node connections were damaged in their patients.

Atrioventricular node structure and function. Our findings have implications concerning the physiology of the normal AV node. The degree of damage to the compact AV node did not correlate well with the degree of impairment of anterograde conduction. However, impairment of anterograde AV node conduction was proportional to the length of the dissection. These findings suggest that the site of entry to the AV node may influence AV node conduction time (Figs. 7 and 8).

It is clear that during sinus rhythm in the normal heart, atrial impulses enter the AV node by way of the most anterior atrionodal connections (within 1 to 2 mm of the central fibrous body and His bundle) because interruption of these connections prolonged the AH interval. Conduction through these connections results in a relatively short conduction time. Maps of excitation during sinus rhythm indicated that these connections were activated before the posterior atrionodal connections. When the anterior connections are destroyed, atrial

impulses must then enter the AV node through more posterior connections, which results in a longer AH interval (Fig. 8). We cannot determine whether the increase in conduction interval results from a longer course when impulses enter by way of more posterior connections or whether the posterior atrionodal inputs have intrinsic properties of slower conduction. Holman and colleagues (20,21) also observed an increase in AH interval after the creation of cryolesions in the perinodal atrium in a canine model. However, because these investigators placed cryolesions at nine sites surrounding the AV node, they could not localize the site of lesions causing an increase in the AH interval.

Similarly, during ventricular pacing at relatively slow rates, the anterior atrionodal connections are the preferred route of exit from the AV node. Maps of atrial excitation during VA conduction demonstrate that the site of earliest atrial excitation is at the apex of Koch's triangle at the site of the most anterior atrionodal connections. Moreover, dissection of these connections resulted in a change in the pattern of retrograde atrial excitation.

Relation of these findings to catheter ablation techniques. Since the advent of catheter ablation techniques using radiofrequency energy for the cure of AV junctional reentrant tachycardia, surgical cure is rarely attempted (12,13,22–24). Two methods have been developed, one in which radiofrequency energy is applied close to the His bundle (12,13) and another in which energy is applied near the coronary sinus orifice in an attempt to ablate the slow pathway (22–24). The surgical technique described here appears analogous to the former technique, although surgical dissection may create a less extensive lesion because destruction of the fast pathway rarely occurs, whereas this is common with the radiofrequency technique (4,12,13,19).

Study limitations. A possible limitation of this study is the use of a canine model. Sustained AV junctional reentrant tachycardia was not inducible in any dog. It may be argued that the use of the canine model does not accurately reflect the effects of the same surgical procedure in humans with AV junctional reentrant tachycardia. However, others (25) have reported that the AV node in dogs and that in humans have many similarities. Moreover, in an anatomic study in a human with AV junctional reentrant tachycardia (26), extranodal pathways were not present, and the AV node appeared similar to those of humans without AV junctional reentrant tachycardia. In addition, endocardial mapping of atrial activation in humans with AV junctional reentrant tachycardia or dual pathways (4,11) has revealed similar exit sites to those found in the dogs in this study. Thus, although not perfect, the canine AV node is a suitable model for the purposes of this study.

Our histologic methods may also be criticized. To confirm that the anterior part of the AV node is completely isolated from the atrium, it would be preferable to perform three-dimensional reconstructions using 5-μm sections. Although we examined only every 10th section (intersection distance 50 μm), we believe it is unlikely that transitional fibers contacted the compact AV node because a thick band of fibrous tissue separated the AV node from the overlying atrium and because activation mapping showed that the site of exit from the node during retrograde conduction was altered. Another limitation of this study is that the region of interest was divided into 5-mm blocks before sectioning; thus, valuable information may have been lost. However, we attempted to minimize this loss by cutting the blocks in such a way that the compact AV node was wholly within one of these blocks. Finally, Racker (25) recently reported that the use of longitudinal sections may allow better definition of the atrionodal connections into discrete bundles of fibers. The use of similar sections may have allowed us to better define the nature of the surgical lesion.

Conclusions. The results of this study indicate that the surgical procedure disconnects the anterior part of the AV node from the overlying atrium but that some direct damage to the AV node does occur. Interruption of these connections is likely to be the predominant mechanism of cure of AV junctional reentrant tachycardia in humans by this procedure. Denervation of the AV node is probably not the mechanism of cure. The atrionodal connections closest to the His bundle are the preferred route of conduction in the normal heart during either AV or VA conduction. Destruction of these connections may modify AV conduction, which suggests that the site of entry of impulses into the AV node may influence AV node conduction time.

We gratefully acknowledge the assistance of Erica Eves, Edward Freitas, Nurten Goktekin, Peter Grant, Gabrielle Hancock, Leslie Hines, Anne Madden, Eve O'Connor, Damodar Pokhrel, Bill Sinai, Alan Steirn, Sara Tasseron, Elisabeth Wallace, Ian Weir and the staff of the Animal Care Department, Westmead Hospital.

References

1. Barker PS, Wilson FN, Johnston FD. The mechanism of auricular paroxysmal tachycardia. Am Heart J 1943;26:435–45.
2. Bigger JT, Goldreyer BN. The mechanism of paroxysmal supraventricular tachycardia. Circulation 1970;42:673–88.
3. Denes P, Wu D, Dhingra RC, Chuquimia R, Rosen KM. Demonstration of dual A-V nodal pathways in patients with paroxysmal supraventricular tachycardia. Circulation 1973;48:549–55.
4. Ross DL, Johnson DC, Denniss AR, Cooper MJ, Richards DA, Uther JB. Curative surgery for atrioventricular junctional ("AV nodal") reentrant tachycardia. J Am Coll Cardiol 1985;6:1383–92.
5. Cox JL, Holman WL, Cain ME. Cryosurgical treatment of atrioventricular node reentrant tachycardia. Circulation 1987;76:1329–36.
6. Holman WL, Hackel DB, Lease JG, Ikeshita M, Cox JL. Cryosurgical ablation of atrioventricular nodal reentry: histological localization of the proximal common pathway. Circulation 1988;77:1356–62.
7. Suzuki F, Kawara T, Sato T, et al. Fast-slow form of "atrioventricular nodal" reentrant tachycardia suggesting atrial participation in the reentrant circuit. Am J Cardiol 1989;63:1413–6.
8. Fujimura O, Guiraudon GM, Yee R, Sharma AD, Klein GJ. Operative therapy of atrioventricular node reentry and results of an anatomically guided procedure. Am J Cardiol 1989;64:1327–32.
9. McGuire MA, Lau KC, Johnson DC, Richards DA, Uther JB, Ross DL. Patients with two types of atrioventricular junctional (AV nodal) reentrant tachycardia. Evidence that a common pathway of nodal tissue is not present above the reentrant circuit. Circulation 1991;83:1232–46.
10. Keim S, Werner P, Jazayeri M, Akhtar M, Tchou P. Localization of the fast

and slow pathways in atrioventricular nodal reentrant tachycardia by intraoperative ice mapping. Circulation 1992;86:919–25.

11. McGuire MA, Bourke JP, Robotin MC, et al. High resolution mapping of Koch's triangle using sixty electrodes in humans with atrioventricular junctional ("AV nodal") reentrant tachycardia. Circulation 1993;88(Pt 1): 2315–28.
12. Goy JJ, Fromer M, Schlaepfer J, Kappenberger L. Clinical efficacy of radiofrequency current in the treatment of patients with atrioventricular node reentrant tachycardia. J Am Coll Cardiol 1990;16:418–23.
13. Lee MA, Morady F, Kadish A, et al. Catheter modification of the atrioventricular junction using radiofrequency energy for control of atrioventricular nodal reentry tachycardia. Circulation 1991;83:827–35.
14. Johnson DC, Nunn GR, Meldrum-Hanna W. Surgery for atrioventricular node reentry tachycardia: the surgical dissection technique. Semin Thorac Cardiovasc Surg 1989;1:53–7.
15. Becker AE, Anderson RH. Morphology of the human atrioventricular junctional area. In: Wellens H, Lie K, Janse M, editors. The Conduction System of the Heart: Structure, Function and Clinical Implications. Philadelphia: Lea & Febiger, 1976:263–86.
16. Tawara S. Das Reitzleitungssystem des Saugetierherzens. Jena: Gustav Fischer, 1906:116.
17. Sung RJ, Waxman HL, Saksena S, Juma Z. Sequence of retrograde atrial activation in patients with dual atrioventricular nodal pathways. Circulation 1981;64:1059–67.
18. Paulsen PK, Thomsen PE, Mortensen PT, Albrechtsen O. Curative surgical treatment of atrioventricular junctional re-entrant tachycardia by perinodal dissection. Eur J Cardiothorac Surg 1989;3:397–400.
19. Ruder MA, Mead RH, Smith NA, Gaudiani VA, Winkle RA. Comparison of pre- and postoperative conduction patterns in patients surgically cured of atrioventricular node reentrant tachycardia. J Am Coll Cardiol 1990;17:397–402.
20. Holman WL, Ikeshita M, Lease JG, Smith PK, Ferguson TB, Cox JL. Elective prolongation of atrioventricular conduction by multiple discrete cryolesions. A new technique for the treatment of paroxysmal supraventricular tachycardia. J Thorac Cardiovasc Surg 1982;84:554–9.
21. Holman WL, Ikeshita M, Lease JG, Ferguson TB, Lofland GK, Cox JL. Alteration of antegrade atrioventricular conduction by cryoablation of peri-atrioventricular nodal tissue. Implications for the surgical treatment of atrioventricular nodal reentry tachycardia. J Thorac Cardiovasc Surg 1984; 88:67–75.
22. Haissaguerre M, Gaita F, Fischer B, et al. Elimination of atrioventricular nodal reentrant tachycardia using discrete slow potentials to guide application of radiofrequency energy. Circulation 1992;85:2162–75.
23. Jackman WM, Beckman KJ, McClelland JH, et al. Treatment of supraventricular tachycardia due to atrioventricular nodal reentry by radiofrequency ablation of slow-pathway conduction. N Engl J Med 1992;327:313–8.
24. Kay GN, Epstein AE, Dailey SM, Plumb VJ. Selective radiofrequency ablation of the slow pathway for the treatment of atrioventricular nodal reentrant tachycardia. Evidence for involvement of perinodal myocardium within the reentrant circuit. Circulation 1992;85:1675–88.
25. Racker DK. Atrioventricular node and input pathways: a correlated gross anatomical and histological study of the canine atrioventricular junctional region. Anat Rec 1989;224:336–54.
26. Scheinman MM, Gonzalez R, Thomas A, Ullyot D, Bharati S, Lev M. Reentry confined to the atrioventricular node: electrophysiologic and anatomic findings. Am J Cardiol 1982;49:1814–8.